Available online at www.sciencedirect.com
ScienceDirect
ELSEVIER
Ceramics International 36 (2010) 1423–1427
CERAMICS INTERNATIONAL
www.elsevier.com/locate/ceramint

Effects of trace of Bi_2O_3 addition on the morphology of strontium ferrite particles

Liang Qiao, Bin Xu, Qiaoqin Xi, Jingwu Zheng, Liqiang Jiang *

College of Chemical Engineering and Materials Science, Zhejiang University of Technology, Hangzhou 310014, People's Republic of China

Received 30 November 2009; received in revised form 15 December 2009; accepted 30 January 2010
Available online 1 March 2010

Abstract

A strontium ferrite powder added with trace of Bi_2O_3 was prepared by the conventional high-temperature solid phase reaction. The effects of Bi_2O_3 addition on the morphology of Sr-ferrite particles fired at different temperatures and times were investigated. The results show that a small quantity of Bi_2O_3 addition accelerates the reaction of SrO and Fe_2O_3 to form SrM ferrite and obviously improves the morphology and size of the strontium ferrite particles. A possible mechanism was proposed to interpret the influence of trace of Bi_2O_3 addition on the morphology of strontium ferrite particles.

PACS : 74.62.bf; 75.50.Dd; 74.62.Dh; 75.60.−d

Keywords: Bi_2O_3; Strontium ferrite; Morphology; Mechanism

1. Introduction

M-type strontium hexaferrite $SrFe_{12}O_{19}$ is one of the most important hard magnetic materials, widely used for permanent magnets and magnetic-recording media, due to its fairly large magnetocrystalline anisotropy, high Curie temperature, relatively large magnetization, as well as excellent chemical stability and corrosion resistivity [1,2].Currently, strontium ferrites were prepared by traditional ceramic process with $SrCO_3$ and Fe_2O_3 as the main raw material in the industry. Besides the chemical composition [3] and sintering process [3–7], the additive is also important here, because it influences the microstructure and magnetic properties of SrM ferrites. Bi_2O_3 used in preparing soft magnets as one sintering additive has been widely studied. Liu et al. [8] found that Bi_2O_3 is able to promote the densification LiZn ferrite. High Bs and lower Hc can be achieved due to the liquid-phase sintering under the action of Bi_2O_3. Yu et al. [9] also revealed that Bi_2O_3 enriched in the grain boundary area promotes the densification of MnZn ferrite during the sintering. In the field of injection molding hard magnets, the shape of nearly spherical ferrite particles are needed in order to meet the requirement of good flowability. The action mechanism of trace of Bi_2O_3 on the morphology of Sr-ferrite particles is rarely reported though it has attracted great interest to improve the magnetic properties of the sintered ferrites [10–14]. In this paper, the strontium ferrite powder was prepared by conventional solid-phase synthesis process with trace of Bi_2O_3 ($\leq$1 wt%) and a probable mechanism was proposed to explain the effects of Bi_2O_3 on the morphology of the strontium ferrite particles.

2. Experimental procedure

The starting materials used were $SrCO_3$, Fe_2O_3, and Bi_2O_3. SrM ferrite of composition $SrFe_2O_{19} + xBi_2O_3$ ($x = 0$, 0.5, 1, 1.5 wt%) were prepared by a solid-state reaction method (defined $x = 0$ as pure sample). Stoichiometric mixtures of oxides were thoroughly ground in a porcelain mortar, then precalcined for 0–2 h in air within the temperature range of 900–1150 °C in corundum crucibles.

SEM (Hitachi S-4700) was used to observe the particle morphology of the as-received powders. The contents of Bi and Sr in the samples were characterized by XRF (ARL ADVANT'X).

---

* Corresponding author. Tel.: +86 571 88320142; fax: +86 571 88320142.
E-mail address: jiliqi@zjut.edu.cn (L. Jiang).

doi:10.1016/j.ceramint.2010.02.003

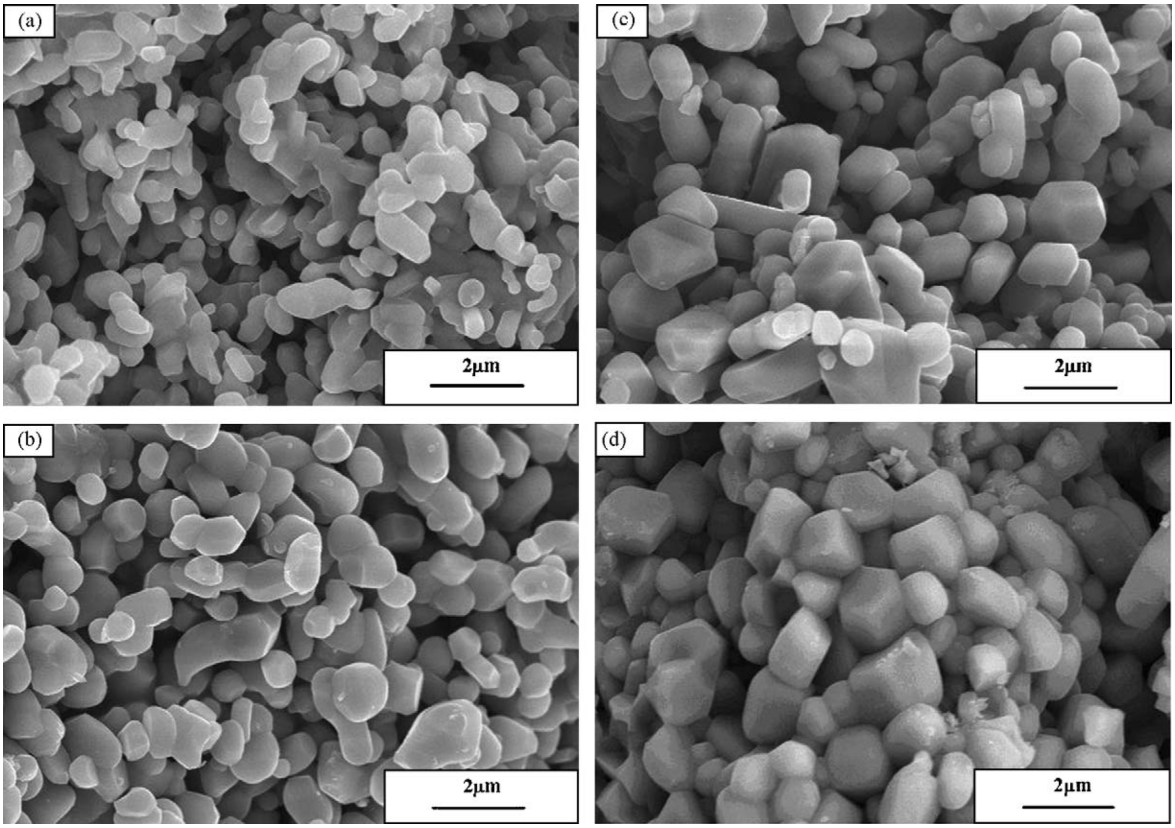

Fig. 1. Morphology of strontium ferrites preheated at 1050 °C for 2 h with (a) $x = 0$, (b) $x = 0.5$, (c) $x = 1$ and (d) $x = 1.5$.

3. Results and discussion

Fig. 1 illustrates the typical SEM photographs of the sintered specimens. It can be seen from this figure that the sizes of SrM ferrite particles obviously increase as the Bi_2O_3 contents increase from 0 to 0.5 wt%, which implies that trace of Bi_2O_3 is able to stimulate the particle growth of SrM ferrites. However, the particle sizes are not obviously becoming larger with the Bi_2O_3 contents continuing to rise except that the particles get together and display a sintered morphology.

Fig. 2 shows the morphology of strontium ferrites prepared at different temperatures with $x = 0$ and 1. When the firing temperature is 900 °C, the particle size of the sample with $x = 0$ is small and irregular compared with the sample with $x = 1$. As the calcination temperatures increase, the particles of both samples begin to grow. However, the particle size of the sample with 1 wt% Bi_2O_3 is larger and has better spherical shape compared with the sample without Bi_2O_3. This indicates that the addition of Bi_2O_3 is not only favorable to the particle growth but also the particle uniformity. When the calcination temperature reaches 1050 °C, the as-received Sr-ferrite particles with $x = 1$ have the sizes of about 1.2 μm with homogeneous spherical shapes. The sizes continue to increase to over 1.5 μm as the calcination temperature rises to 1150 °C. However, most particles with no Bi_2O_3 addition only have the size of about 0.8 μm even though the firing temperature increases to 1150 °C as shown in Fig. 2(c). In addition, it is also found that the particles of the sample with $x = 0$ join each other and display serious agglomeration tendency with vague particle boundaries. However, the particles of the sample added with trace of Bi_2O_3 decrease the juncture and have clear boundaries when the calcination temperature raised from 900 °C to 1150 °C as shown in Figs. 2 and 1(c).

It has already been reported that Bi^{3+} can enter into the crystal lattice of ferrites and form a series of $AFe_{12-x}Bi_xO_{19}$ (A = Ba, Sr) phases [10–12]. However, it is difficult for Bi^{3+} to enter into the crystal lattice of ferrites if the firing temperature is below 1100 °C [13]. Hence, under the conditions of trace of Bi_2O_3 addition and lower firing temperatures, Bi_2O_3 comes into being liquid phase outside the crystal lattice, which has an effect on the formation and morphology of Sr-ferrites.

The state of liquid phase containing Bi is indefinite during the synthesis process of the strontium ferrites. XRD was used to check the Bi_2O_3 phase. But the amounts of Bi_2O_3 in the experiments are too small to be detected by the XRD measurements. There is also no obvious liquid phase to be observed in the microphotographs of the fired samples with Bi_2O_3 addition as shown in Figs. 1 and 2. Assuming the liquid from 1 wt% Bi_2O_3 homogeneously disperses and covers the surface of the ferrite particles with the size of 1.5 μm, the thickness of liquid layer calculated is about 3 nm which cannot be shown in the SEM photographs. XRF was used to detect the Bi existence in the fired samples calcined at 1050 °C for 2 h. Table 1 displays the Bi contents of the sample with 1 wt% Bi_2O_3 addition by using XRF. The results show that $w(Bi^{3+})/w(Sr^{2+})$ is 0.088 which implies the Bi existence

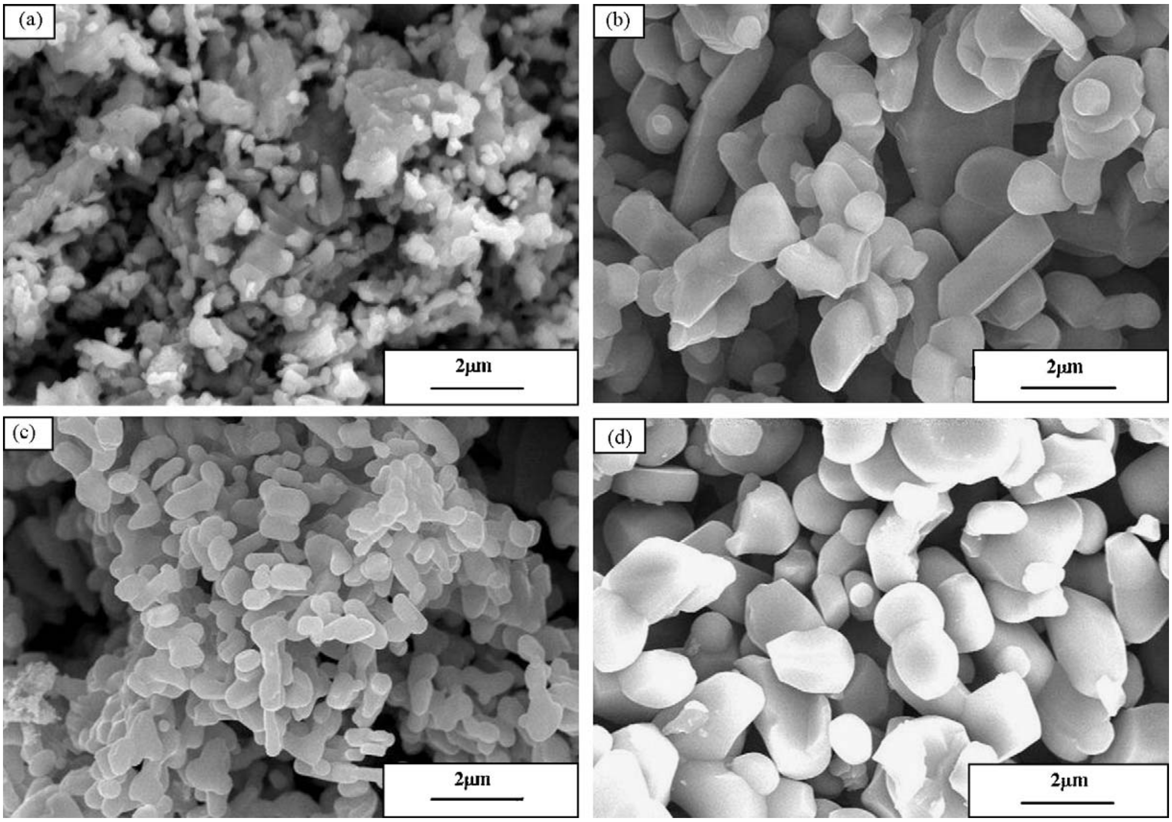

Fig. 2. SEM photographs of the samples with different x calcined at different temperatures for 2 h: (a) 900 °C, $x = 0$, (b) 900 °C, $x = 1$, (c) 1050 °C, $x = 0$ and (d) 1050 °C, $x = 1$.

Table 1
Sr and Bi contents in the Sr-ferrites fired at 1050 °C for 2 h.

Process	Sr^{2+} (wt%)	Bi^{3+} (wt%)	$w(Bi^{3+})/w(Sr^{2+})$
A: before acid washing	10.67	0.936	0.088
B: after acid washing	6.88	0.62	0.09

even if it is a little lower than the original proportion of 0.113 calculated from the raw materials. It can be defined that the liquid existing in the samples is Bi_2O_3 or other second phases through measuring the Bi contents of the powder after acid washing since Bi_2O_3 is easy to resolve into the acid and eliminated as well-known. The same powders washed using 25% hydrochloric acid was detected by XRF and the results were also listed in Table 1. It can be seen that $w(Bi^{3+})/w(Sr^{2+})$ is 0.09, which is in agreement with the Bi content before acid washing considering the measuring error. This indicates that the liquid is not the single Bi_2O_3 melt during the firing process. It is possible that a new liquid containing Bi forms during the firing and plays an important role on the morphology of ferrite particles.

According to the morphology change as shown in Figs. 1 and 2, a possible mechanism is proposed here to explain the action of the liquid containing Bi. Figs. 3 and 4 show the sketch map of the ferrite formation when $x = 0$ and 1. In the case of $x = 0$, there exists a solid reaction between SrO and Fe_2O_3. As the reaction goes on, the particles join together since Sr-ferrite layers form between SrO and Fe_2O_3 particles and become large as shown in Fig. 3(b). When the solid phase reaction finishes, the resultant forms an agglomeration and shapes into vague particle boundaries as displayed in Fig. 3(c), which is similar with the factual morphology shown in Figs. 1 and 2. In the case of $x = 1$, Bi_2O_3 firstly forms liquid above its melting point (825 °C) and disperses in the SrO and Fe_2O_3 mixture as shown in Fig. 3(d). As the firing temperature increases, SrO and Fe_2O_3 begin to dissolve into the Bi_2O_3 liquid [12] and form a middle liquid containing Bi_2O_3–SrO–Fe_2O_3 compounds. When the concentrations of Sr, Fe and O ions reach to the composition of $SrFe_{12}O_{19}$ phase, SrM phase is precipitated from the Bi–Sr–Fe–O liquid. This causes the new solution of SrO and Fe_2O_3 outside the liquid as shown in Figs. 3(e) and 4. Repeatedly, the larger the SrM particle, the thinner the liquid layer covering it. The Sr-ferrite finally stops growing when SrO and Fe_2O_3 outside the liquid layer are completely consumed. The reaction between SrO and Fe_2O_3 is greatly improved since it occurs in the Bi–Sr–Fe–O liquid in comparison with that between two solid phases. The Sr-ferrite particles grow into near spherical shapes because there is the liquid layer on the surface of them as shown in Fig. 3(f). Since the liquid layer is a medium of SrO and Fe_2O_3 solution and SrM precipitation, trace of Bi_2O_3 addition is able to obviously improve the growth of ferrite particles.

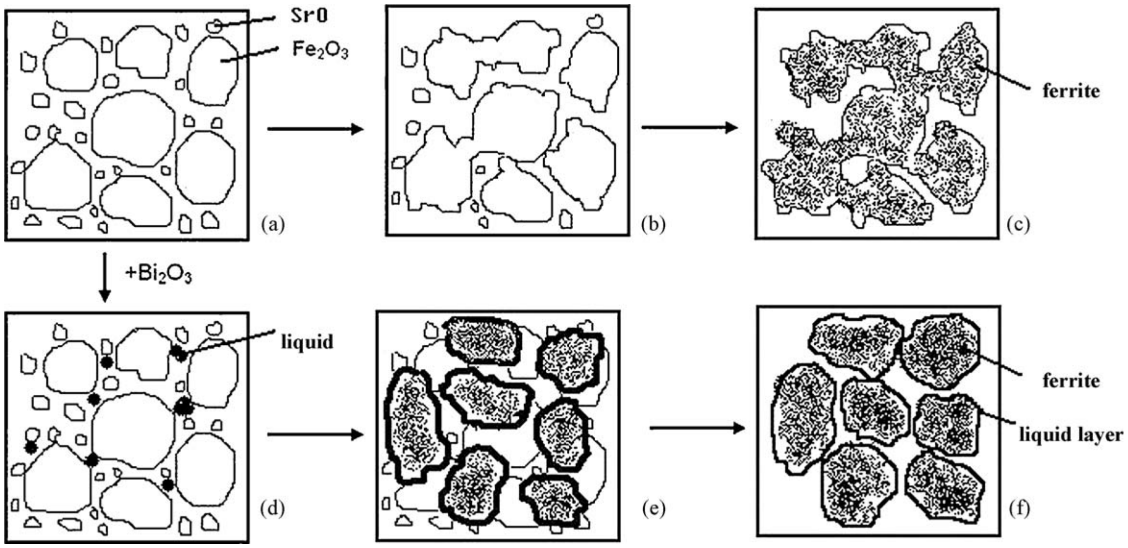

Fig. 3. Sketch map of the change of Sr-ferrite morphology.

The behavior of Bi_2O_3 stimulating the formation of ferrites can be verified by observing the experimental phenomena of the middle state. The samples with $x = 0$ and 1 were fired to 900 °C and then cooled immediately to room temperature with no holding time. It is found that the product with 1 wt% Bi_2O_3 addition becomes black agglomeration and is easily attracted by a strong magnet. Differently, the product with no Bi_2O_3 addition still retains in red and loose state with weak magnetic property like that before the firing process. This implies that SrO and Fe_2O_3 dissolve into the Bi_2O_3 liquid and form SrM phase even at the low temperature of 900 °C.It is known that Bi_2O_3 can improve the grain growth due to a liquid sintering mechanism which is usually described by the solution-precipitation course. In the present experiments, 1 wt% Bi_2O_3 was added in the commercial ferrite powder and then fired at 1050 °C for 2 h to observe the morphology change of the ferrites. As shown in Fig. 5, most fine particles in the fired samples disappear, which indicates that the fine particles dissolve and precipitate on the surface of larger ferrite particles. It can also be seen in this figure that the solution-precipitation course cannot effectively help to form the spherical shape since the precipitation occurs on the surface of the original ferrite particles.In order to compare the solution rate of SrO/Fe_2O_3 mixture in the Bi_2O_3 liquid, the equivalent quantity $SrCO_3/Fe_2O_3$ mixture with mole ratio of 1/6 and the commercial ferrite powder were paved on a layer of Bi_2O_3 powder, and then fired at 900 °C for 2 h. Bi_2O_3 was paved on a layer of Al_2O_3 powder with 2 cm thickness to avoid the corrosion of alumina crucible by the Bi_2O_3 melt. The original and corresponding fired samples were shown in Fig. 6 where the commercial ferrite and $SrCO_3/Fe_2O_3$ mixture powders were signed by A and B symbols respectively. It can

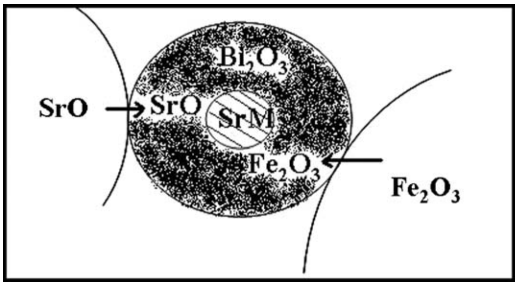

Fig. 4. Sketch map of the liquid action.

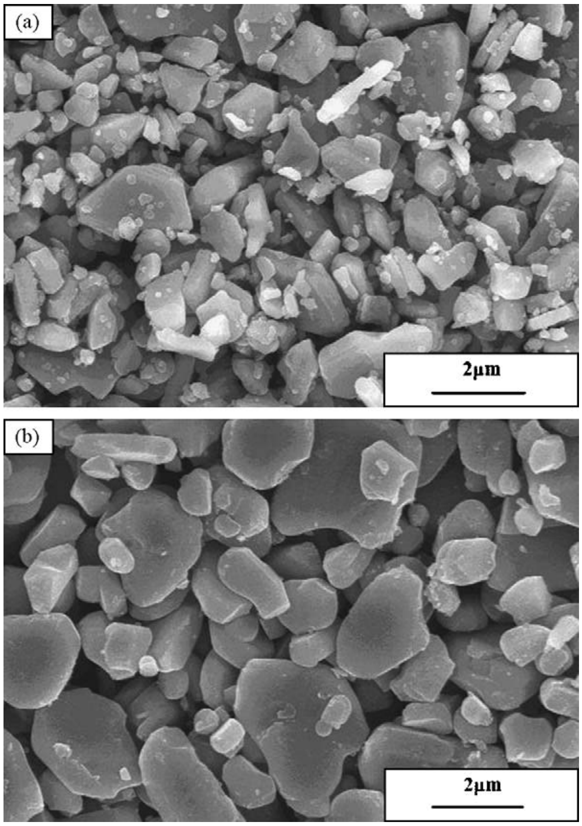

Fig. 5. SEM photographs of commercial Sr-ferrite powders fired at 1050 °C for 2 h with (a) the original state and (b) 1 wt% Bi_2O_3 addition.

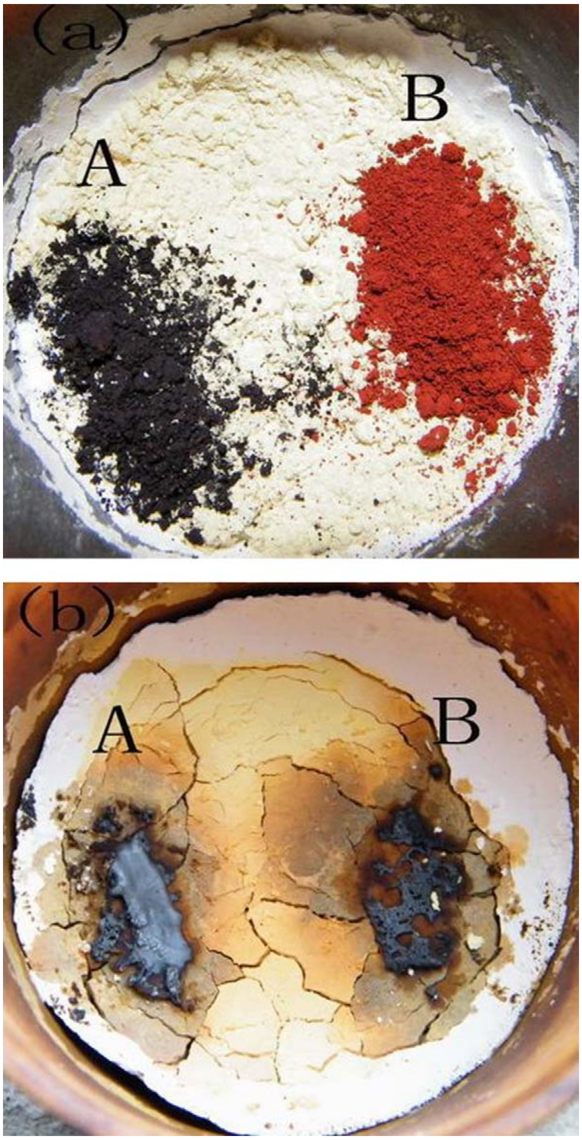

Fig. 6. Photographs of commercial ferrite and $SrCO_3/Fe_2O_3$ mixture powders dissolving into Bi_2O_3 liquid: (a) the original state and (b) fired at 900 °C for 2 h.

be seen that there is a larger solution area and a less remain in B district compared with A district. This indicates that the solution speed of SrO/Fe_2O_3 mixture toward the Bi_2O_3 liquid layer is faster in comparison with the single ferrite powders. Though the solution-precipitation mechanism of ferrite grains widely exists in the sintering of Sr-ferrites in the case of Bi_2O_3 addition, the mechanism of SrO and Fe_2O_3 resolving in Bi_2O_3 liquid and form ferrites is more reasonable in preparing Sr-ferrite powders with near spherical shape as shown in Figs. 3(f) and 4.

4. Conclusions

(1) The addition of trace of Bi_2O_3 improves the particle size and morphology in preparing the Sr-ferrite powders for inject molding. When the calcination temperature is at 1050 °C, the particles of samples with Bi_2O_3 addition are more homogeneous and display a near spherical shape with the size of about 1.2 μm. In the same firing process, the particles are irregular and have a size of about 0.8 μm in the sample without Bi_2O_3 addition.

(2) The action mechanism of trace of Bi_2O_3 on the morphology of ferrite particles is proposed as following: SrO and Fe_2O_3 dissolve in the Bi_2O_3 liquid, and thereafter form SrM phase in it. The liquid layers enwrap the SrM phase and become thinner as SrM phase grows outward. When all the SrO and Fe_2O_3 particles are consumed, Sr-ferrites stop growing and come into being homogeneous particles with near spherical shape.

References

[1] M. Imanura, Y. Ito, M. Fujiki, T. Hasegawa, H. Kubaota, T. Fujiwara, IEEE Trans. Magn. 22 (1986) 1185.
[2] K. Yamamori, T. Suzuki, T. Fujiwara, IEEE Trans. Magn. 22 (1986) 1188.
[3] H. Su, H.W. Zhang, X.L. Tang, Y.L. Jing, Y.L. Liu, J. Magn. Magn. Mater. 310 (2007) 17.
[4] J.H. Jean, C.H. Lee, J. Am. Ceram. Soc. 82 (1999) 343.
[5] N. Rezlescu, L. Sachelarie, E. Rezlescu, C.L. Sava, P. Popa, Ceram. Int. 29 (2003) 107.
[6] B.P. Rao, C.O. Kim, C.G. Kim, Mater. Lett. 61 (2007) 1601.
[7] J.H. Jean, C.H. Lee, Jpn. J. Appl. Phys. 40 (2001) 2232.
[8] C.Y. Liu, Z.W. Lan, X.N. Jiang, Z. Yu, K. Sun, L.Z. Li, P.Y. Liu, J. Magn. Magn. Mater. 320 (2008) 1335.
[9] Z. Yu, K. Sun, L.H. Li, Y.F. Liu, Z.W. Lan, H.W. Zhang, J. Magn. Magn. Mater. 320 (2008) 919.
[10] J. Li, Y. Duan, H. He, D. Song, J. Alloys Compd. 315 (2001) 259.
[11] T. Osotchan, S. Thongmee, I.M. Tang, Thammasat Int. J. Sci. Technol. 4 (1999) 54.
[12] D.D. Zaitsev, P.E. Kazin, Yu.D. Tret'yakov, M. Jansen, Inorg. Mater. 12 (2003) 1319.
[13] S. Ram, J. Magn. Magn. Mater. 80 (1989) 24l.
[14] S. Ram, H. Krishnan, K.N. Rai, K.A. Narayan, Jpn. J. Appl. Phys. 28 (1989) 604.